Characterization of controlling hydrogeochemical processes using factor analysis in Puyang Yellow River irrigation district (China)

Wenjia Wang, Xianfang Song and Ying Ma

ABSTRACT

Groundwater chemistry is diverse and complicated and is regulated by both natural hydrogeochemical and anthropogenic processes. Determining the governing processes and their influence on groundwater chemistry is very important to understand groundwater quality evolution and establish reasonable water management strategies. Main cations (Ca^{2+}, Mg^{2+}, Na^{+}, K^{+}, and Sr^{2+}), anions (Cl^{-}, SO_4^{2-}, HCO_3^{-}, NO_3^{-}, and F^{-}), and SiO_2 and UV254 of 50 shallow groundwater samples were treated and analyzed. Factor analysis combined with ionic ratio and correlation analysis was used to identify the major hydrogeochemical processes responsible for the variation of hydrochemical components. Approximately 76% of the total variance of the data set can be explained by the four factors identified. Composing of Sr^{2+}, Mg^{2+}, Ca^{2+}, and electrical conductivity (EC), Factor 1 accounted for 25.67% of the total variances, and represented groundwater formation background and fundamental water–soil/rock interaction. Factor 2 with high loadings on NO_3^{-}, U(Cl^{-}, SO_4^{2-}, HCO_3^{-}, NO_3^{-}, and F^{-}), and F^{-})254, and F^{-}, was related to anthropogenic activities, especially the release of domestic sewage and industrial effluents. Factor 3 composed of Na^{+}, HCO_3^{-} and EC was interpreted as cation exchange process. Factor 4 explained 15.75% of the total variance, and was attributed to the influence of agricultural activities, especially chemical fertilizer application.

Key words | cation exchange, factor analysis, hydrogeochemical processes, ionic ratio, irrigation district, Yellow River

Wenjia Wang
Xianfang Song (corresponding author)
Ying Ma
Key Laboratory of Water Cycle and Related Land Surface Processes,
Institute of Geographic Sciences and Natural Resources Research, Chinese Academy of Sciences,
Beijing 100101,
China
E-mail: *songxf@igsnrr.ac.cn*

Wenjia Wang
Graduate University of Chinese Academy of Sciences,
Beijing 100049,
China

INTRODUCTION

As one of the most important water resources, groundwater constitutes nearly all usable freshwater resources in the world, if the polar ice caps and glaciers are not considered (Chapman 1996). Groundwater resources have been used for domestic, agricultural, industrial, and/or environmental purposes based on water quality (Prasanna *et al.* 2010). Groundwater quality is a collective result of various factors including natural processes and anthropogenic activities (Rajmohan & Elango 2004). In a natural system, atmospheric deposition, mineral dissolution–precipitation, and cation absorption–desorption processes are the responsible processes for groundwater chemistry. With the rapid increase in population and industrial and agricultural development, anthropogenic activities show increasing influence on the groundwater chemistry and natural geochemical processes. As such, changes in groundwater chemistry compositions caused by irrigation should not be neglected (Deshmukh *et al.* 2011; Qin *et al.* 2011) because large amounts of irrigation water not only change local hydraulic conditions but also transport chemical substances from irrigation water and the vadose zone into the groundwater aquifer, thereby altering the groundwater chemical compositions of groundwater.

doi: 10.2166/nh.2016.233

In irrigation districts, groundwater chemistry is influenced by the hydrochemical processes that occur in the natural system and by irrigation water quality. As surface irrigation water usually has relative low salinity, infiltration of irrigation water largely dilutes the groundwater. However, in some cases, infiltration of irrigation water may also increase groundwater salinity. Affected by strong evaporation before and during the infiltration process, surface irrigation during the summer season may increase groundwater salinity (Kass *et al.* 2005). Contaminated irrigation water with high salinity also contributes to the increase in groundwater salinity. In shallow groundwater areas, a large amount of irrigation return flow and less groundwater abstraction raise the groundwater level and result in groundwater salinization caused by strong phreatic water evaporation. In addition to the influence of irrigation on general groundwater salinity, irrigation activities also affect the spatial distribution of groundwater salinity through the redistribution of soluble salts in a phreatic aquifer (Surinaidu 2016). With the influence of geographic conditions, permeability of soil, and thickness of unsaturated zone, irrigation water infiltration can alter the original groundwater flow, and chemical substances dissolved in groundwater usually move with the water flow and concentrate in low-lying areas and downstream regions. Together with the overall change in groundwater salinity, chemical compositions also change significantly in irrigation regions. Most of the chemical modifications can be attributed to the base-exchange reactions which are primarily controlled by the initial chemical composition of the irrigation water. Normally, infiltration of fresh irrigation water with high Ca^{2+} and less Na^{+} is usually accompanied by cation-exchange process in groundwater involved in the uptake of Ca^{2+} and release of Na^{+} into water, resulting in Na^{+}/Cl^{-} increase in groundwater. Carbonate dissolution in the unsaturated zone can be induced by the removal of Ca^{2+} from the water (Appelo & Postma 2005). However, because domestic wastewater is enriched with Na^{+}, irrigation of water contaminated by domestic sewage leads to reverse cation exchange. Excess Na^{+} and K^{+} are absorbed by clay minerals, whereas Ca^{2+} and Mg^{2+} are released into the water (Stigter *et al.* 1998; Appelo & Postma 2005; Kass *et al.* 2005).

To identify the dominant hydrochemical processes in groundwater and to assess their contributions to geochemical evolution in irrigation areas, different methods, including hydrogeochemical diagrams such as Piper trilinear nomograph and Gibbs diagram (Gibbs 1970), ionic ratios method, multivariate statistical analysis (Lawrence & Upchurch 1982; Munoz-Carpena *et al.* 2005; Panda *et al.* 2006; Cloutier *et al.* 2008), and inverse and forward geochemical modeling have been intensively used. Field sampling and investigation at basin scale usually produce a large number of data sets including different physical and chemical indicators. Identifying the dominant hydrochemical processes based on visual inspection and descriptive statistics only can be difficult. Eigenvector techniques including factor analysis (FA) are efficient dimensionality reduction methods conducted by extracting hidden common factors from a large amount of highly correlated variables. These methods are widely used to determine the dominant processes that may regulate the hydrogeochemical and physical components of groundwater (Dragon 2006; Panda *et al.* 2006; Yang *et al.* 2010; Surinaidu 2016).

The Yellow River (YR) is the second longest river in China and the most sediment filled river on Earth. Along the YR and its tributaries, irrigation districts with different scales are densely distributed. Due to sediment deposition in the watercourse of the flow path, the world famous 'suspended river' is gradually formed in the lower reaches of the YR, with the riverbed 3–8 m above ground. The location of the suspended river allows YR to replenish the groundwater at both sides all year around. The irrigation district located in the lower YR is the largest gravity irrigation area in China, with an accumulated amount of water of 294.95 billion m^3 diverted from the YR since the 1970s and an average annual irrigation area of 20,956 km^2 since the 1990s (Wang 2007). Therefore, studying the impact of surface water irrigation on groundwater quality and the controlling hydrochemical processes in irrigation districts are important for managing water resources and securing the safeness of drinking water in these districts.

The objective of this paper is to determine the major factors controlling groundwater chemistry using FA, interpret the corresponding hydrogeochemical processes combined with ionic ratios, and identify the area of influence and its intensity by each hydrogeochemical process based on factor scores.

MATERIALS AND METHODS

Study area

PYR irrigation district is located in the northeast of Henan province, adjacent to Shandong and Hebei provinces (Figure 1). The district covers an area of about 3,150 km^2 and has a population of over 2.89 million. This district belongs to the continental monsoon climate zone, with a mean annual temperature of 13.3 °C, and most of the precipitation occurs between July and October with an annual average precipitation of 554 mm. The district is divided by the Jindi River, with the northern region belonging to the Haihe River Basin and the southern area belonging to the YR Basin.

PYR is an important base for grain production and petrochemicals with a water-deficit region of 220 m^3 water resources per capita, which is only one tenth of the country's average. It has nearly 90 tributaries belonging to the YR and Haihe River systems, respectively, most of which are medium and small rivers. Among them, YR, Jindi River (JDH), and Weihe River (WH), spanning the study area from west to east, are the most important ones of the river systems, and the amount of available passing water is 854 million m^3.

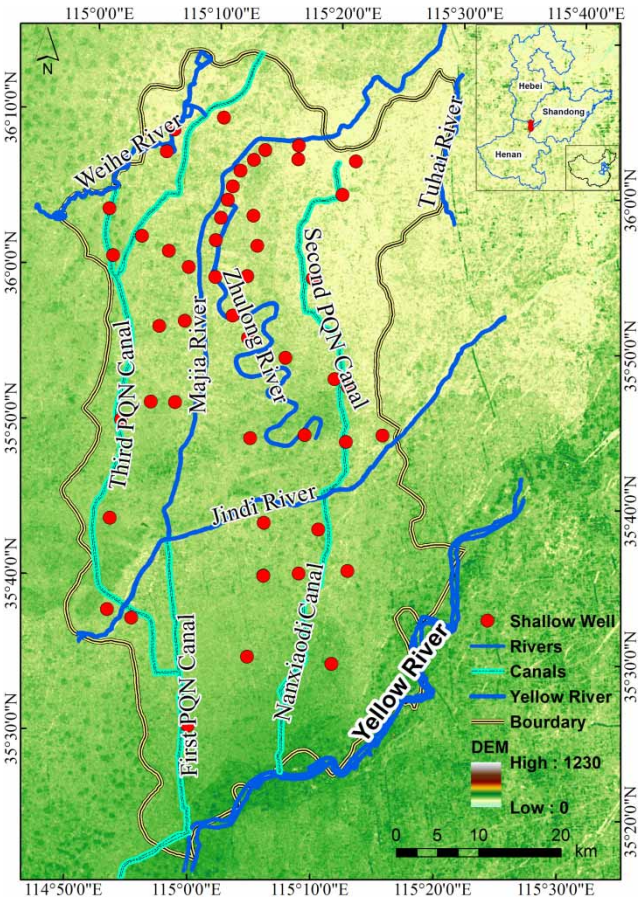

Figure 1 | Location of the sampling sites: (1) the location of the sampling shallow wells; (2) main rivers and irrigation canals.

To relieve pressure on local water resources and better utilize the unique geographical advantages of the YR, which is suspended over the ground in its lower reaches, local government began diverting the water from the YR for farmland irrigation during the 1950s. However, a deficiency in facilities supporting irrigation and blind development during the Great Leap Forward period caused the 'stop irrigation' period in the YR because of extensive land salinization (Wang 2007). During the establishment and operation of the first Puyang-Qingfeng-Nanle (PQN) irrigation canal in 1986, the PYR irrigation region officially entered the modern irrigation period. With the construction of the second and third PQN irrigation canals and relevant facilities in the past 30 years, the amount of water diverted from the YR has increased to around 500 million m^3 per year. Across the YR and Haihe River basin, artificial canals in the irrigation district are mainly distributed from south to north.

The PYR irrigation district is superposed over the Dongpu sag, which is a Cenozoic extensional rift basin located in the southwest part of Bohai Bay basin. This sag is controlled by the master fault, the Lanliao fault, and is a large rollover structure over the listric Lanliao fault. Within the study area, the longest fault is the Changyuan fault, which is the boundary of Dongpu sag and Neihuang uplift, whereas the second longest fault is the YR fault, which is situated between Changyuan and Lanliao faults.

As a part of the YR alluvial plain, PYR irrigation district is mainly composed of river deposits with minerals consisting of quartz, feldspar, and a small quantity of melanocratic minerals. The loose bed thickness of the quaternary deposits ranges from 350 to 400 m, and the stratum structure consists of overlapping sand, silt, and clay soil. Groundwater is widely distributed in the study region. Based on aquifer properties and hydraulic connection of the different layers, groundwater can be divided into two different aquifer

groups. The shallow aquifer consists of pore phreatic water and feeble-confined water above 150 m, and the deep aquifer is pore-confined water between 150 and 350 m beneath the surface. Thus far, private domestic water and irrigation water have mainly depended on shallow phreatic aquifers above 150 m, whereas centralized urban water supply mainly depends on deep confined aquifers. Oil-field exploitation in the east of Puyang even reached 350 m locally. The hydraulic connection between phreatic aquifer and confined aquifer is negligible because of the presence of claypan with weak permeability. The depth to the water table in a phreatic aquifer varies significantly in the study area, fluctuating between 2 and 8 m in the YR basin. However, in the Haihe River basin, groundwater depth reaches >20 m. To illustrate the general flow field in this area, phreatic groundwater levels were contoured (Figure 2). In general, the flow direction of groundwater in the study area was from south to north. The hydraulic conductivity of the phreatic aquifer changed between 0.57 and 4.63 m day^{-1}. The specific yield of unconfined aquifers varied from 0.03 to 0.12. The main recharge sources of groundwater in unconfined aquifers are infiltration recharge of precipitation and irrigation water. In the YR basin, lateral seepage of the YR is also an important recharge source. In addition, lateral groundwater inflow from outside of the study region is another recharge source that cannot be ignored in areas with large hydraulic gradients. Evaporation is the major way of discharging in areas with depth of groundwater levels less than 4 m, which is usually the critical depth of phreatic water evaporation. In most of the PYR irrigation region with deeper water tables, artificial exploitation was the dominant mode of discharging. In addition, lateral outflow and leakage discharge are important discharge patterns. With the development of well-irrigated agriculture and industry in

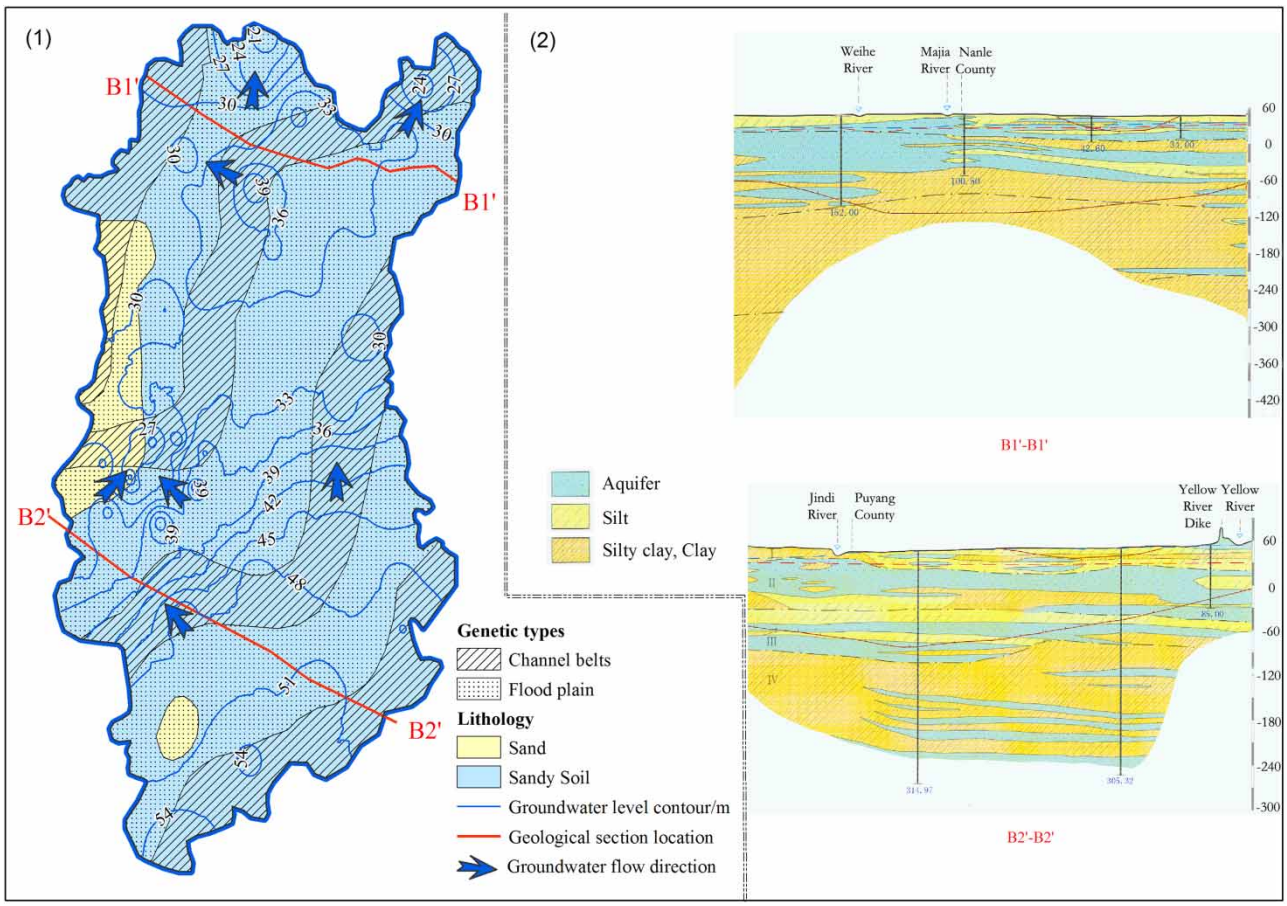

Figure 2 | Hydrogeological map of the study area: (1) geological genetic types and lithology; (2) geological section maps.

the past few decades, the PQN depression cone, which is the biggest depression cone in the North Henan Plain, was formed gradually in the late 1990s due to the massive exploitation of groundwater with funnel area of 1,857 km^2 (Rao 2009).

Sample collection and analysis

To better understand the hydrochemical composition of shallow groundwater, 50 groundwater samples were collected uniformly in the PYR irrigation district within the first week in August 2013, and were taken from shallow wells with depth <100 m. Two 50 mL polyethylene bottles with watertight caps were used to store the filtrated water (0.45 μm Millipore membrane filter) for cations (Ca^{2+}, Mg^{2+}, Na^{+}, K^{+}, Sr^{2+}) and anions (Cl^{-}, SO_4^{2-}, NO_3^{-}, F^{-}) analysis, and another 100 mL was used for determining bicarbonate concentration. All samples were stored at 4 °C after bottling.

Electrical conductivity (EC), pH, and water temperature were measured *in situ* via a previously calibrated multiparameter portable meter (HACH40d, USA). HCO_3^{-} concentration was determined according to acid–base titration method on the day of sampling before filtration. UV254 was measured by ultraviolet spectrophotometer (DR5000, USA).

The major ions of water samples were treated and analyzed in the Physical and Chemical Analysis Center Laboratory of the Institute of Geographic Sciences and Natural Resources Research (IGSNRR), Chinese Academy of Sciences (CAS). Cations (Ca^{2+}, Mg^{2+}, Na^{+}, K^{+}, and Sr^{2+}) and SiO_2 were measured by inductively coupled plasma optical emission spectrometry (ICP-OES). Anion (Cl^{-}, SO_4^{2-}, NO_3^{-}, and F^{-}) analysis was carried out on ion chromatography (IC). The limitation of detection of ICP-OES and IC are 1 μg/L and 1 mg/L, respectively. Analytical precision for major ions was within 1%. For all water samples, ion balance error was <5% (Appelo 1996).

Statistical analysis

The FA model assumes that for a specific variable, its variance is composed of the linear function of several common factors and a special factor unique to the original variable. The basic purpose of FA is to extract the common factors from a large number of highly correlated variables and calculate the factor loadings for each variable and factor scores for each sample. The premise of using FA is that variables are highly correlated, making it possible to extract common factors. In addition, enough samples are available to ensure the stability of the results of FA.

To facilitate FA, and eliminate the influence caused by differentiation of data units and dimensionality, the data were standardized to produce a normal distribution of all variables prior to FA (Davis 2002). The first step of FA was to generate the correlation coefficients matrix of the initial data set, in which most correlation coefficients were greater than 0.3. The derived factors, which were linear combinations of the original variables, were extracted by the principal component analysis method. Factor extraction was done using the criteria whose eigenvalues were greater than 1. The first factor obtained explains the largest number of variance, and the following factors explain repeatedly the smaller parts of the variance. To understand and interpret the derived factors, orthogonal rotation of the initial factors to terminal factor solutions was done with Kaiser's Varimax scheme. This method maximized the variance of the loadings on the factors and hence adjusted them to be near ±1 or zero. Factor loadings showed how the factors characterized the variables, with high factor loadings (close to 1 or −1) indicating the strength of the relationship (positive or negative) between a variable and a factor describing that variable (Dragon 2006). The sum of squares of factor loadings for each variable is called communality and reflects the proportion of the total variability of the variables accounted for by the factoring.

To evaluate the correctness of the FA, namely, to examine if the correlation coefficients among the variables are sufficiently high to be reduced by the factor analytical model, the Bartlett test of sphericity and the Keiser–Meyer–Olkinn (KMO) measure of sampling were computed. KMO test was used to examine partial correlation between variables, with values ranging between 0 and 1; the closer a value to 1, the stronger was the partial correlation that indicates the effectiveness of FA. Usually, when the value was greater than 0.5, conducting FA was approved. When the KMO value was greater than 0.8, it is considered excellent for FA, whereas a value less than 0.5 often indicated

that the data set was not appropriate. Bartlett test of sphericity was used to determine whether the different variables were strongly correlated; $P > 0.05$ meant that the data followed the test of sphericity, and the variables were highly correlated, indicating their suitability for FA and vice versa.

Factor scores were calculated by summing the products of a series of factor score coefficients and their corresponding data. Factor scores greater than +1 usually indicated intense influence by the process; factor scores less than 0 suggest virtually the process represented by factor that has no effect, whereas near-zero scores reflected areas limitedly affected by the process. Data obtained from the *in situ* measurement and laboratory analysis were used as variable inputs for FA. FA was performed using Statistical Product and Service Solutions 19.0.

As one of the most useful multivariate statistics methods, successful application of FA largely relies on the reasonable and professional interpretations of the extracted results. Ionic ratio was used to distinguish the different hydrogeochemical processes and identify the major dissolved minerals responsible for different ion concentrations in water. Na^+/Cl^- and $(Ca^{2+} + Mg^{2+})/(HCO_3^- + SO_4^{2-})$ mole ratios were used to identify the major hydrochemical processes and compositions of minerals that are the source of Na^+ and $Ca^{2+} + Mg^{2+}$ in groundwater, respectively (Meybeck 1987). For the cation exchange process that exists in most groundwater systems, Na^+/Ca^{2+} was the commonly used indicator. Joint use of FA and ionic ratio method could be promising in characterizing the dominant hydrogeochemical processes in groundwater; on one hand, ionic ratios of waters with different factors helped in the interpretation of extracted factors; on the other hand, factor scores for water samples contributed to the further understanding of the distribution feature, especially the extremum and outliers in the ionic ratio scatter plots. In addition, spatial mapping of factor scores that represented the governing hydrogeochemical processes was used to identify the intensity of influence and extent of specific hydrogeochemical processes.

RESULTS

Basic characteristics of groundwater chemistry

Basic statistics of the chosen chemical parameters are listed in Table 1. In general, the dominant cation in groundwater was HCO_3^- with median value of 340.1 mg/L, and the dominant anion was Na^+ with median value of 153.1 mg/L. The coefficients of variance (CV) is the ratio of standard deviation to the mean value of a variable. CV shows the extent of variability in relation to the mean of variables, and is advantageous in allowing comparisons among variables that differ in units

Table 1 | Descriptive statistics of hydrochemical parameters

Parameters	Minimum	Maximum	Median	Standard deviation	Coefficient of variance/%
EC, μs/cm	924.0	4,580.0	1,661.5	758.7	41.86
HCO_3^-, mg/L	203.3	559.2	340.1	81.6	23.35
SO_4^{2-}, mg/L	12.8	298.3	95.0	58.3	58.26
Cl^-, mg/L	27.9	418.2	98.0	75.8	63.50
NO_3^-, mg/L	0.3	222.0	2.4	40.6	219.97
F^-, mg/L	0.232	4.372	0.649	0.636	83.68
Ca^{2+}, mg/L	30.6	173.9	83.4	33.1	37.71
Mg^{2+}, mg/L	32.3	213.9	72.8	31.9	40.86
Na^+, mg/L	37.8	578.9	153.1	117.8	65.70
K^+, mg/L	0.396	6.983	1.69	1.320	66.10
SiO_2, mg/L	8.9	21.4	17.31	3.2	19.08
Sr^{2+}, mg/L	0.7	4.3	1.6	0.6	34.41
UV254	0.005	0.051	0.018	0.012	56.69

and ranges. Among these variables, NO_3^- showed the highest CV, which is probably affected by point contamination, whereas SiO_2 and HCO_3^- demonstrated the smallest CVs indicating the similar formation background of the groundwater in the study area. Correlation analysis results are shown in Table 2. EC was significantly correlated with most variables, with the highest correlation coefficient of 0.803 computed for Na^+. Mg^{2+}, Ca^{2+}, and Sr^{2+} were highly and positively correlated, among which the correlation coefficient between Mg^{2+} and Sr^{2+} was greater than 0.9, possibly indicating their common source. No significant correlation was observed between Mg^{2+} and Sr^{2+}, and Na^+, which suggests that Na^+ had a different source from the other major cations. As for the anions, Cl^-, SO_4^{2-}, and NO_3^- were significantly correlated, whereas HCO_3^- which is usually assumed to be a product of mineral weathering, was significantly and negatively correlated with Cl^-, and no obvious relationship was found between SO_4^{2-} and HCO_3^-. Beyond certain limits, NO_3^- and UV254 are often regarded as indicators of anthropogenic pollution (Fenech *et al.* 2012); these two parameters were significantly and positively correlated in the study, with a correlation coefficient greater than 0.5.

The hydrochemical types of groundwater in the PYR are complicated by the samples dispersedly distributed in the Piper trilinear diagram (Figure 3). Most of the samples' concentrates in the middle inverted triangle zone of Ca^{2+}-Mg^{2+}-($Na^+ + K^+$) trilinear diagram showed no significantly advantageous cations, and the others fell into the zone with $Na^+ + K^+$ as their advantageous cations. As for the anions, HCO_3^- was the dominant ion in most samples, and a few sites had Cl^- as their major anion. In addition, we observed that with the increase in EC, the dominant anion in groundwater changed from HCO_3^- to Cl^-, and the predominant cations switched from Ca^{2+} and Mg^{2+} to Na^+.

FA analysis results

Computed values of the Bartlett test of sphericity which were greater than 0.5 and the KMO results with sig. <0.001 suggest that the data set was suitable for FA. Table 3 shows the Varimax rotated factor matrix consisting of the component factors, loadings of variables on each factor, and percentage of data variance explained by each factor. Four extracted factors described 76.20% of the data set variance. Factor 1

Table 2 | Results of bivariate correlation analysis

	EC	F^-	Cl^-	SO_4^{2-}	HCO_3^-	Ca^{2+}	K^+	Mg^{2+}	Na^+	SiO_2	Sr^{2+}	NO_3^-	UV254
EC	1.000												
F^-	−0.564**	1.000											
Cl^-	0.611**	−0.340*	1.000										
SO_4^{2-}	0.680**	−0.337*	0.521**	1.000									
HCO_3^-	0.127	0.142	−0.409**	−0.121	1.000								
Ca^{2+}	0.464**	−0.807**	0.286*	0.297*	−0.216	1.000							
K^+	0.110	−0.371**	0.315*	0.157	−0.165	0.240	1.000						
Mg^{2+}	0.610**	−0.427**	0.234	0.358*	0.231	0.543**	0.082	1.000					
Na^+	0.803**	−0.209	0.449**	0.523**	0.283*	−0.008	−0.001	0.208	1.000				
SiO_2	−0.618**	0.275	−0.498**	−0.512**	0.054	−0.112	−0.119	−0.069	−0.670**	1.000			
Sr^{2+}	0.454**	−0.400**	0.247	0.198	0.119	0.554**	0.126	0.878**	0.034	0.014	1.000		
NO_3^-	0.557**	−0.627**	0.395**	0.396**	−0.139	0.564**	0.346*	0.391**	0.280*	−0.567**	0.283*	1.000	
UV254	0.542**	−0.617**	0.431**	0.503**	−0.143	0.469**	0.380**	0.287*	0.349*	−0.541**	0.161	0.652**	1.000

*Correlation is significant at the 0.05 level (two-tailed).
**Correlation is significant at the 0.01 level (two-tailed).

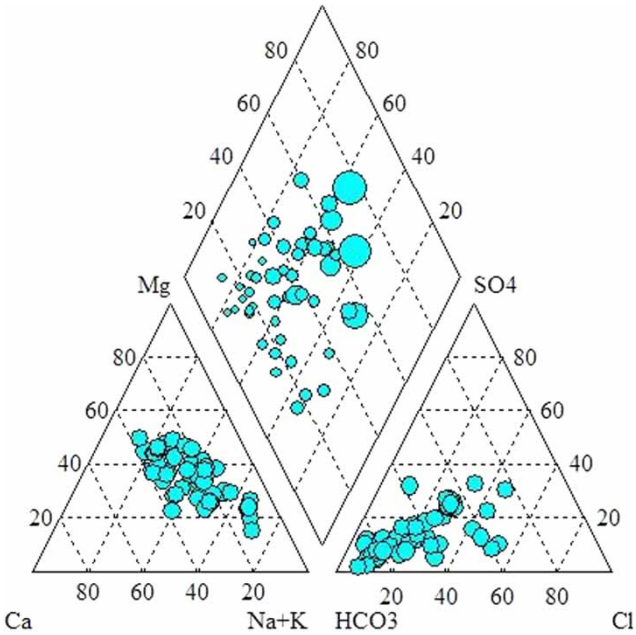

Figure 3 | Trilinear diagram showing composition ratios for shallow groundwater water, solid circle radii is proportional to EC ranging from 500 to 2,699 μs/cm.

showed the highest factor loadings on Sr^{2+} (0.928) and Mg^{2+} (0.909), high factor loading on Ca^{2+} (0.749) and EC (0.696), and it explained 25.67% of the total variance (Figure 4(a)). Factor 2, which explained 18.76% of the total variance, exhibited high positive loadings on NO_3^- (0.825) and UV254 (0.824) and negative loading on F^- (−0.594). Factor 3 accounting for a similar amount of variance to Factor 2, showed high and positive loadings on both Na^+ (0.791) and HCO_3^- (0.761) (Figure 4(b)). Factor 4 explained 15.75% of the total variance, with major positive loadings on Cl^- (0.717) and K^+ (0.686). Communalities were the results of sums of factors' squares, which meant that the proportion of variance can be explained by the extracted factors, and the rest is defined as a specific factor; both contribute to the variance of variables. Calculated results of communalities suggested that over than 65% of the variances for all variables except for SO_4^{2-} and K^+ can be explained by the four extracted factors, with EC (0.943) and Mg^{2+} (0.927) having the greatest communalities higher than 0.9.

DISCUSSION

Ion concentrations in groundwater are usually affected by multiple hydrogeochemical processes including mixing and evaporation processes, mineral dissolution and deposition,

Table 3 | Results of the factor analysis (after varimax rotation)

Parameter	Factor 1	Factor 2	Factor 3	Factor 4	Communalities
Sr^{2+}	**0.928**	−0.086	0.094	0.056	0.881
Mg^{2+}	**0.909**	0.067	0.306	−0.054	0.927
Ca^{2+}	**0.749**	0.447	−0.259	0.105	0.838
EC	0.696	0.341	0.555	0.187	0.943
NO_3^-	0.000	**0.825**	0.156	0.100	0.716
UV254	0.152	**0.824**	0.071	0.220	0.755
F^-	−0.462	−0.594	0.357	0.379	0.836
Na^+	0.304	0.296	**0.791**	0.181	0.839
HCO_3^-	0.043	−0.147	**0.761**	−0.478	0.830
Cl^-	0.361	0.061	−0.169	**0.717**	0.677
K^+	−0.060	0.047	−0.022	0.686	0.477
SiO_2	0.113	−0.427	−0.442	−0.643	0.804
SO_4^{2-}	0.359	0.318	0.139	0.366	0.383
Eigenvalues	3.337	2.439	2.082	2.047	
% of variance explained	25.67	18.76	16.02	15.75	
Cumulative % of variance	25.67	44.43	60.45	76.20	

Factor loadings >0.7 are marked by bold font.

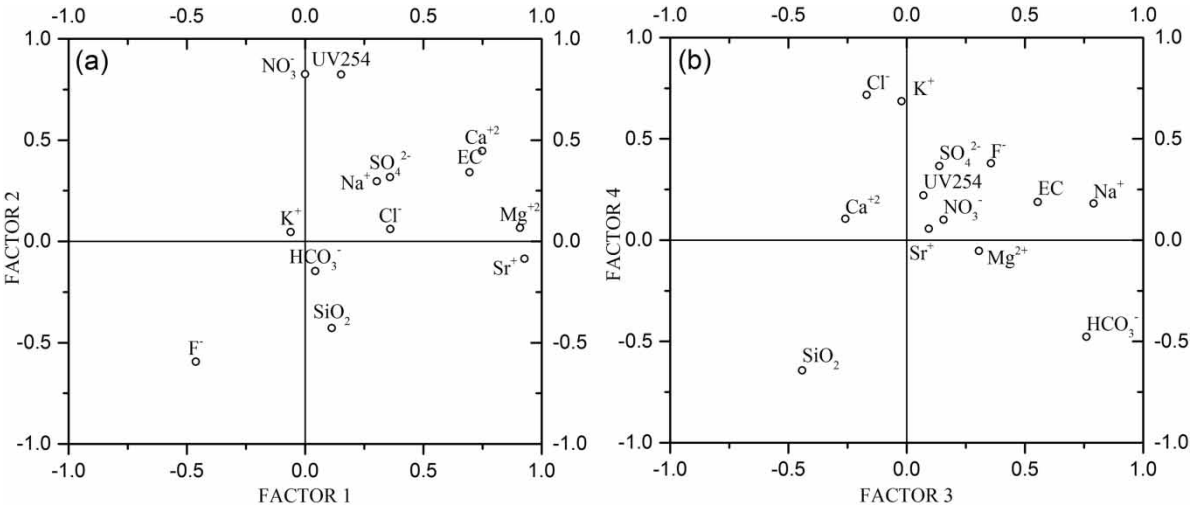

Figure 4 | Factor loadings of all of variables for: (a) factor 1 – factor 2 loadings; (b) factor 3 – factor 4 loadings.

rock weathering, ion exchange and other possible anthropogenic inputs. Gibbs diagram, which is initially used for discovering the major mechanisms controlling global surface water chemistry, is one of the most useful and widely used tools used to discriminate various hydrogeochemical processes (Gibbs 1970). Both of the scatter plots of the weight ratios of $Na^+/(Na^+ + Ca^{2+})$ and $Cl^-/(Cl^- + HCO_3^-)$ versus total dissolved solids (TDS) showed that rock weathering was the main mechanism controlling chemical compositions in groundwater (Figure 5). In the diagram of

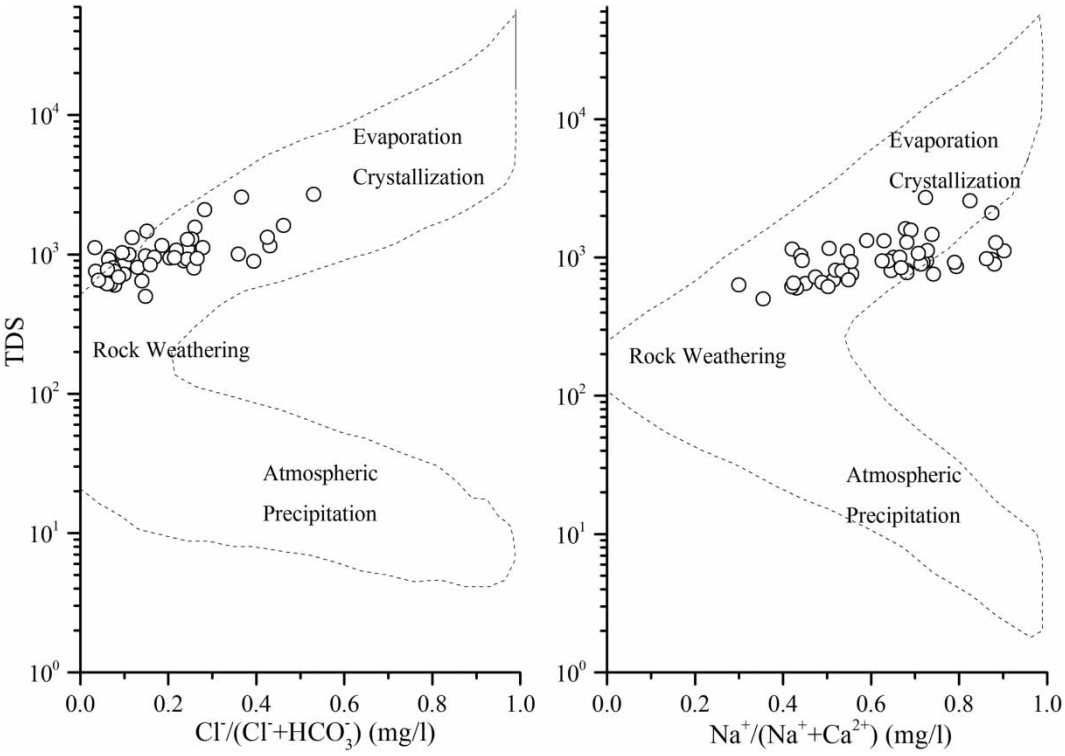

Figure 5 | Gibbs diagram: (a) TDS versus $Cl^-/(Cl^- + HCO_3^-)$ and (b) TDS versus $Na^+/(Na^+ + Ca^{2+})$.

$Cl^-/(Cl^- + HCO_3^-)$ versus TDS, the weight ratios of $Na^+/(Na^+ + Ca^{2+})$ varied from less than 0.3 to over 0.9, without significant change in TDS values, indicating that cation exchange may play a role in the variation. Cation exchange, which results in the increase in Na^+ and decrease in Ca^{2+} in groundwater, usually causes no significant changes in TDS because every 2 mmol L^{-1} of Na^+ (46 mg/L) released into groundwater was approximately 1 mmol L^{-1} of Ca^{2+} (40 mg/L) that was absorbed.

Mineral weathering and dissolution

EC generally describes the total concentration conditions of anions and cations in groundwater and is influenced by natural hydrochemical processes as well as anthropogenic activities, among which evapotranspiration plays an important role. Phreatic water evaporation increases the EC value through concentrating ions. Assuming that no mineral species precipitation was present during the evaporation process, the Na^+/Cl^- ratio was expected to be constant because evaporation should not alter the ionic ratio (Jankowski & Acworth 1997). Therefore, the plot of Na^+/Cl^- ratio versus EC was expected to produce a horizontal line. In this study, Na^+/Cl^- mole ratio varied from over 10 to less than 1, samples with F1 scores >0 mainly distributed along the $r(Na^+)/r(Cl^-) = 1$ line with higher EC values, while the others with F1 scores <0 were distributed perpendicularly to this line with EC values less than 2,000 μs/cm (Figure 6). This suggested that

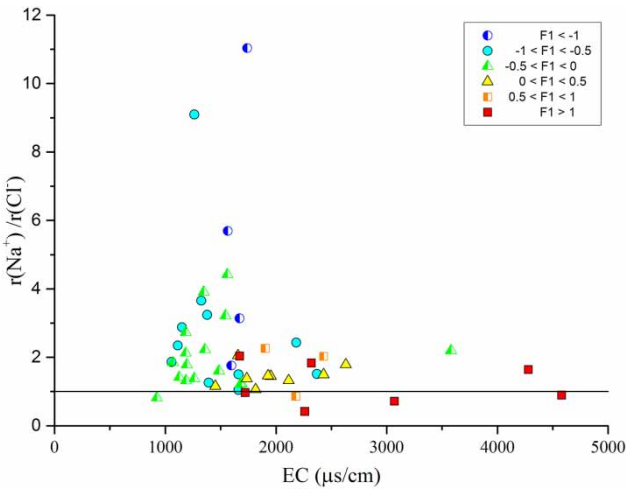

Figure 6 | Scatter plot of $m(Na^+/Cl^-)$ versus EC.

samples completely unaffected or slightly affected by factor 1 had considerable excess sodium compared to chloride, indicating that the evaporation process was possibly not the dominant process controlling groundwater chemistry, especially in water samples with lower EC values.

Ca^{2+}, Mg^{2+}, and Sr^{2+} are all alkali earth metals with similar chemical properties. As the main cations in natural groundwater, Ca^{2+} and Mg^{2+} are usually derived from the dissolution-infiltration of weathered rock, which reflects the signatures of natural water recharge and water–soil/rock interaction. Sr^{2+} is a minor component in natural groundwater due to the low solubility of celestite ($SrSO_4$) and strontianite ($SrCO_3$) in water. Dissolved Sr^{2+} in groundwater comes mainly from the atmospheric deposition and dissolution of Sr-bearing minerals. Correlation analysis results showed that Ca^{2+}, Mg^{2+}, and Sr^{2+} were positively correlated with each other, indicating that they possibly came from the same source, or they were controlled by the same geochemical process. Therefore, Factor 1 can be regarded as a fundamental process that reflects host mineral compositions and intensity of water–rock interactions. In the process of water–rock interaction, Ca^{2+} and Mg^{2+} mostly originated from the dissolution of carbonate mineral or other minerals containing Ca^{2+} and Mg^{2+}. Comparison of the equivalent proportions of $Ca^{2+} + Mg^{2+}$ versus $SO_4^{2-} + HCO_3^-$ is commonly used to infer the sources of Ca^{2+} and Mg^{2+}. In this study, most samples fell below the 1:1 line, and samples with F3 scores <0 were closely distributed around the 1:1 line, while samples that fell away from the 1:1 line usually had high F3 scores (Figure 7), suggesting a considerable deficit of $Ca^{2+} + Mg^{2+}$ compared with $SO_4^{2-} + HCO_3^-$. This result implies two possible reasons: one is excess alkalinity produced by silicate weathering reactions, which also produces Na^+ and K^+; and the other is deficit of $Ca^{2+} + Mg^{2+}$ due to chemical reactions that consume Ca^{2+} and Mg^{2+}, such as the cation exchange process (Cerling & Pederson 1989). To differentiate these two possible reasons for the deficit of Ca^{2+} and Mg^{2+}, identifying in detail the sources of Na^+ in water was necessary because both hydrogeochemical processes result in excess Na^+ rather than Cl^-.

Cation exchange process

Major sources for sodium in groundwater include halite dissolution, sodium silicate weathering, cation exchange

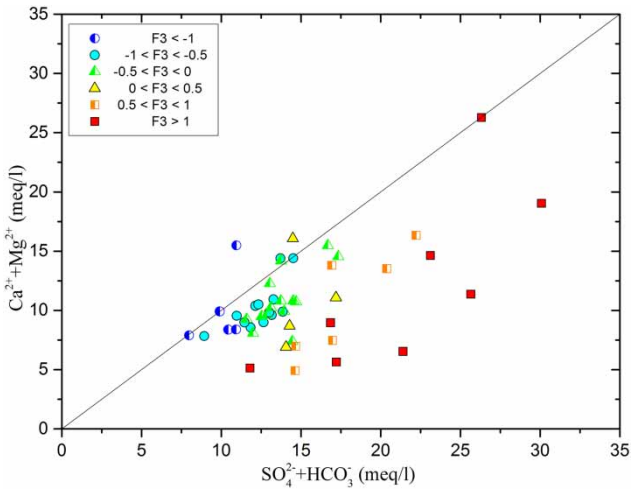

Figure 7 | Scatter diagram of r ($Ca^{2+} + Mg^{2+}$) versus r ($HCO_3^- + SO_4^{2-}$) with 1:1 line.

and anthropogenic inputs. If sodium in groundwater is mainly derived from halite dissolution, the Na^+/Cl^- molar ratio should be approximately equal to 1. In this study, samples with F3 scores <0 were distributed closely along the 1:1 line (Figure 8), indicating sodium in these samples probably derived from halite dissolution. Most samples, especially samples with F3 scores >0 fell above the 1:1 equaline of Na^+ versus Cl^- (Figure 8), which indicates that dissolution of salt rock was not the only source for sodium in groundwater and the hydrogeochemical process represented by Factor 3 should be mainly responsible for excess sodium in groundwater. Samples above

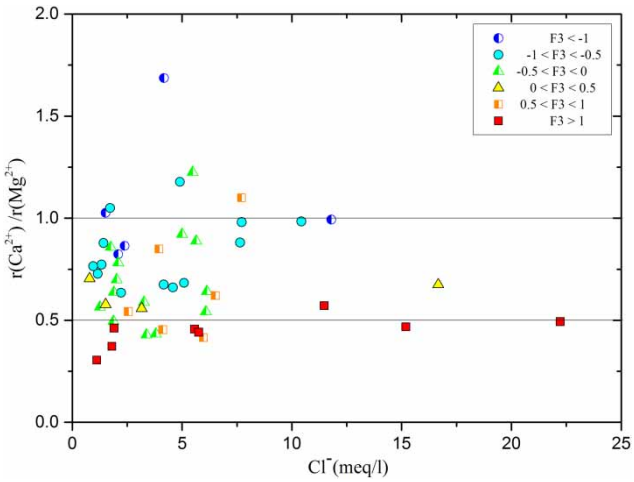

Figure 8 | Scatter plot of r (Na^+) versus (Cl^-) with 1:1 line.

the 1:1 equaline indicated the presence of excess Na^+ compared with Cl^-, which was usually interpreted as a result of silicate mineral weathering (Meybeck 1987), and the reaction of feldspar with carbonic acid with water also released large amounts of HCO_3^- (Rogers 1989). From these functions below, we deduced that the sodium and alkalinity molar ratio should be around 1 when water subjected to silicate weathering was the major sodium source. In addition, large amounts of sodium and bicarbonate ions produced by silicate mineral weathering can increase the total ion content and result in increased EC values. In this study, small correlation coefficient between sodium and bicarbonate implied that albite weathering may not be the main source of excess sodium in groundwater. Samples with high Na^+/Cl^- molar ratios usually have EC values of less than 2,000 μs/cm, and downward trend in Na^+/Cl^- ratio was obviously observed with the increase in EC (Figure 6), further illustrating that silicate weathering is not the major cause of excess sodium in groundwater.

$$2.33NaAlSi_2O_8 + 8.64H_2O + 2CO_2 \leftrightarrow Na_{0.33}Al_{2.33}Si_{3.6}O_{10}(OH)_2 + 2Na^+ + 2HCO_3^- + 3.32H_4SiO_4$$

$$2NaAlSi_3O_8 + 11H_2O + 2CO_2 \leftrightarrow Al_2Si_2O_5(OH)_4 + 2Na^+ + 2HCO_3^- + 4H_4SiO_4$$

Another important source for excess sodium in groundwater is cation exchange process which occurs between groundwater and its ambient clay mineral. This reaction exchanges only cations and is not accompanied by an increase in the anion content (Cerling & Pederson 1989). Moreover, because sodium preferentially replaces calcium ion in water, waters with cation exchange as their major sodium sources usually result in a decrease in Ca^{2+}/Mg^{2+} molar ratio. As shown in Figure 9, samples with greater Factor 3 scores had the smallest Ca^{2+}/Mg^{2+} molar ratio, while samples with Factor 3 scores <0 generally had higher Ca^{2+}/Mg^{2+} ratios, which further verified that cation exchange process represented by Factor 3 preferentially exchanged calcium other than magnesium in water with sodium absorbed on clays, resulting in a decrease of much

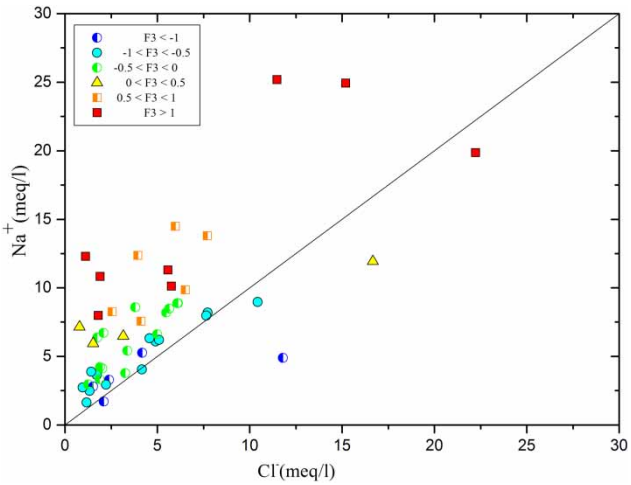

Figure 9 | Scatter diagram of r (Ca^{2+})/r(Mg^{2+}) versus r (Cl^{-}).

more calcium than magnesium.

$$Na_2 - clay + Ca^{+2} = Ca - clay + 2Na^{+}$$

In this study, no obvious change was observed in EC with the increase in the Na^{+}/Cl^{-} molar ratio, which suggests that excess sodium and total ion content have no significant relationship. If cation exchange is mainly responsible for excess sodium in groundwater, the samples should form a line with a slope of -1 in the scatter plot of $Ca^{2+} + Mg^{2+} - HCO_3 - SO_4^{2-}$ versus Na^{+}-Cl^{-} (Rajmohan & Elango 2004). The water samples in the study area formed a line with the equation, $y = -0.8762*x - 7.8878$, with $r^2 = 0.5394$ (Figure 10), which

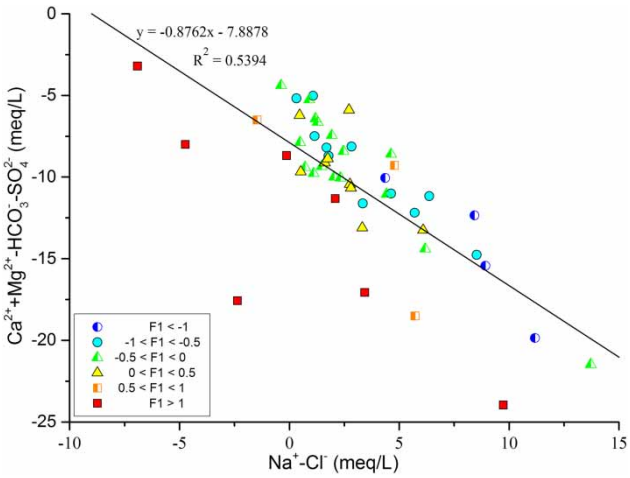

Figure 10 | Scatter plot of r ($Ca^{2+} + Mg^{2+} - HCO_3^{-} - SO_4^{2-}$ versus r (Na^{+}-Cl^{-}) with line −1:1.

indicates that ion exchange was the possible cause of sodium enrichment and calcium depletion in groundwater; the result is consistent with the conclusion in a previous study conducted on the YR alluvial fan (Li *et al.* 2008). Given the establishment of the first PQN irrigation canal in 1986, irrigation history has now spanned almost 30 years. Before the large-scale diverted irrigation from the YR, TDS of shallow groundwater was quite high due to the increase in groundwater level and soil salinization caused by the reservoirs built on the Northern Henan Plain in the 1960s. With the abundant exploitation of groundwater since the 1970s and diverted irrigation from the YR, shallow groundwater was greatly diluted by irrigation water, with a mean TDS of 0.52 g/L in the Huayuankou sampling site (data obtained from the period 1960–2000) (Chen *et al.* 2003). The dominant anion and cation in the YR water were bicarbonate and calcium, respectively. Long-term diverted irrigation supplies sufficient calcium ion which causes the release of large amounts of sodium absorbed on clay minerals into the water and becoming the dominant cation.

Influence of anthropogenic activities

Nitrate in groundwater is naturally found within the environment as part of the nitrogen cycle; however, its ever-increasing concentration makes nitrate a ubiquitous contaminant of natural water resources (Fenech *et al.* 2012). Agricultural activities, including fertilizer and manure application in farmland, are probably the most significant anthropogenic sources of nitrate in groundwater. Environmental land use conflicts and the arbitrary discharge of factory wastewater and domestic sewage without reasonable treatment are other possible sources of nitrate. UV254 in this paper was used as the surrogate parameter in terms of organic matter content because of its significant correlation with chemical oxygen demand (COD) and total organic carbon, which are the common indicators of organic pollution. As one of the most important petroleum and gas bases in China, Zhongyuan oilfield is located in Puyang County, which makes the infiltration of hazardous organic substances into the groundwater possible. Therefore, Factor 2, which has high loadings on NO_3^{-} and UV254, reflects the influence of anthropogenic activities. Except for the high and positive loadings on NO_3^{-} and

UV254, Factor 2 also exerts high and negative loading on F^-. Fluoride in groundwater receives widespread attention because consumption of water with fluoride concentration above 1.5 mg/L results in acute to chronic dental fluorosis and skeletal fluorosis (Brindha & Elango 2011). Fluoride in groundwater is mainly derived from the dissolution of fluoride-bearing minerals, such as fluorspar, fluorapatite, cryolite, and hydroxylapatite, and its concentration is affected by many factors, including the availability and solubility of fluoride minerals, groundwater flow velocity, temperature, pH, and calcium concentration in groundwater. Previous study in China suggests that most groundwaters with high fluoride concentration are located in low-lying areas with slow groundwater runoff, shallow groundwater table, and strong evaporation, which prolong the water–rock interaction and concentrate the fluorine content in groundwater. Therefore, negative loading of Factor 2 on fluoride can be considered as representative of nature groundwater that was unaffected or slightly influenced by the anthropogenic activities, whereas positive loadings of Factor 2 on NO_3^- and UV254 indicate the influence of anthropogenic activities.

Chloride in groundwater is derived from a wealth of sources, of which natural sources include rock–water interactions, seawater intrusion, and minor contributions from atmospheric deposition, and sources related to human activities include road salt, effluent from industrial facilities and municipal septic systems, landfill leachate, and some agricultural chemicals such as potassium chloride (Appelo & Postma 2005). Potassium in natural groundwater can come from the weathering of silicate minerals, orthoclase, microcline, hornblende, muscovite, and biotite in igneous and metamorphic rocks, and the main reason for the increase in potassium concentration is agricultural activities (Hem 1985). Statistical data show that fertilizer usage in Henan province continues to increase year by year. The amount of fertilizer consumption in 2010 was about 2.7 times of that in 1990, of which potash fertilizer consumption increased from 100,000 tons in 1991 to 616,000 tons in 2010 (Peng 2012). Chloride potassium is the largest used potash fertilizer, which accounts for over 90% of total potash fertilizer consumption. Excessive application of chemical fertilizer on farmland can cause percolation of nutrients into the groundwater. In the rainy season, surface runoff takes away most of the remaining fertilizer on farmlands, and lateral seepage of fertilizer-rich surface water is a means for nutrients to infiltrate groundwater. Therefore, Factor 4 with high loadings on Cl^- and K^+ represents the effect of agricultural fertilizer activities on groundwater chemical components.

Spatial distribution of factor scores

The areal distributions of the factor scores (Figure 11) show the spatial variability of controlling hydrochemical processes represented by the extracted factors. Factor 1 composed of EC, Ca^{2+}, Mg^{2+}, and Sr^{2+} represented water-soil/rock interaction intensity and groundwater formation background, which mainly control groundwater chemical compositions. Groundwater samples with high scores of Factor 1 were mainly obtained at places away from rivers and irrigation canals. Most of the samples with high scores were located to the north of Jindi River where groundwater tables decline sharply to over 20 m. Another two samples with exceptional high scores were located north of Jindi River because of the salinity of the land in the area (Tong *et al.* 2005), which makes exploitation difficult and retains water–rock interaction products in groundwater. Water samples collected from sites close to natural rivers and artificial irrigation canals showed the most negative scores, which can be ascribed to the dilution effect of lateral seepage from rivers and irrigation canals.

No obvious trend was observed from the spatial distribution of Factor 2 scores, and samples with high scores were mainly concentrated in urban areas, confluence area of rivers, and administrative boundaries in the lower reaches of rivers. In urban areas, concentrated population and factories, which mainly rely on local wastewater treatment plants, usually produce a large amount of industrial wastewater and domestic sewage. When wastewater treatment capacity is lower than local domestic sewage and wastewater discharge rate, urban sewage discharge without sufficient treatment can cause point-source pollution. In the study area, a large amount of domestic sewage from the western region of Puyang City was discharged into the third PQN canal because of lack of adequate infrastructure and wastewater treatment facilities. In the interaction area of Majia River and Zhulonghe River, with a distance of less than 1 km between, high factor scores possibly resulted

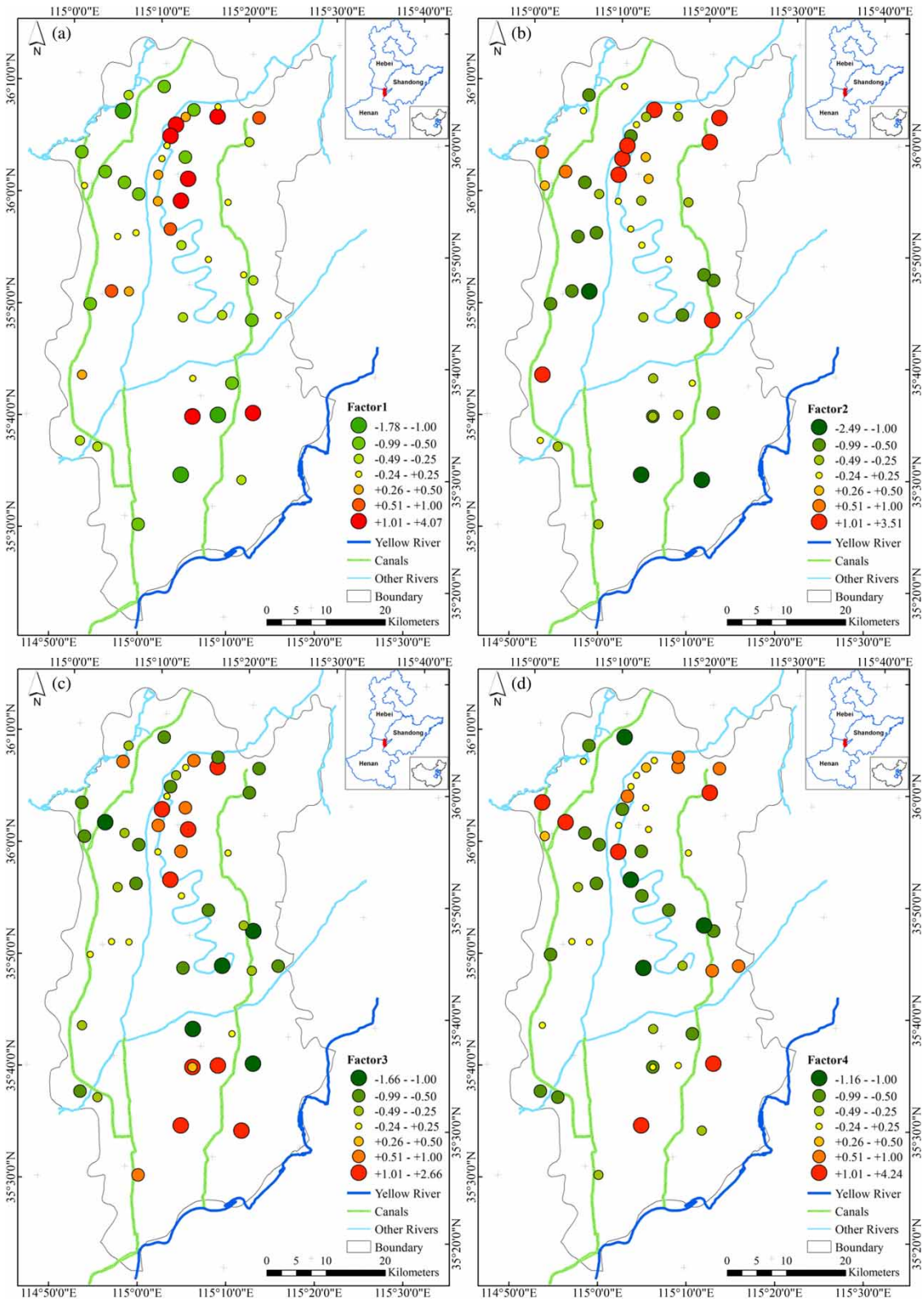

Figure 11 | Spatial distribution of factor scores for (a) Factor 1, (b) Factor 2, (c) Factor 3, and (d) Factor 4.

from infiltration of contaminated river water. The role of stream riparian zones in regulating nutrient transportation has been a major research focus in the past decades (Carlyle & Hill 2001). Due to the allocation mechanism of water resources between Henan and Hebei provinces remaining obscure, regulation sluices over irrigation canals in the administrative boundary are virtually closed throughout the year. Thus, the contaminants are concentrated in this part of the water flow and cause groundwater pollution.

Different from the spatial distribution patterns of Factors 1 and 2, the spatial distribution of Factor 3 was closely related to groundwater level and its flow path. Samples with high scores were mainly located at sites with shallow groundwater depth and high water tables. Such observations were probably obtained because groundwater receives much more recharge from precipitation and YR irrigation water with HCO_3^- and Ca^{2+} as the dominant anion and cation, respectively, in shallow groundwater areas. As indicated in previous research (Li *et al.* 2008), fresh water recharge largely promotes cation exchange process because fresh water supplies large amounts of calcium ions that are readily exchanged with sodium absorbed by clay minerals. Therefore, water samples in fresh water recharge areas usually have a high Na^+/Cl^- ratio (Figure 9), and excess sodium ion can be attributed to the cation exchange process. Compared with samples from the south of Jindi River, samples with high factor scores in the north part close to Zhulonghe River did not receive large amounts of irrigation water, and excess sodium here is mainly due to significant cation-exchange capacity and low permeability of clay-rich soil. Factor 4 scores have a similar spatial distribution pattern to those of Factor 2. Samples with high scores are mainly located in the northmost part of the PYR irrigation district far away from the irrigation gates.

In the YR basin, shallow groundwater depth is from 2 to 8 m. The YR basin is significantly recharged by the lateral seepage of the YR and vertical infiltration of precipitation and irrigation water. The mixing process and dilution effect of the YR reduced groundwater ion concentration, and phreatic water evaporation and transpiration increased groundwater salinity. To prevent groundwater salinization caused by intensive evapotranspiration, groundwater level control and a scientific and reasonable irrigation program is vital for this area. Although significant pollution has not been observed in this area as yet, excessive application of fertilizers and pesticides can potentially threaten groundwater quality. The quality of the YR water also directly affects groundwater quality in this area. In Haihe River basin, which is located away from the YR, groundwater is deeper and lower. A thick vadose zone makes groundwater in this area less susceptible to contamination. However, long-term heavy irrigation still greatly influences groundwater quality to some extent. When the groundwater is contaminated, restoring its quality can be difficult and costly. As the Haihe River basin is located downstream of the irrigation district, irrigation water quality is not only related to the YR water quality, but is also affected by industrial wastewater and domestic sewage that come with the water flow. Due to insufficient sewage treatment capacity in this study region, large amounts of industrial and urban domestic effluents are discharged into natural river courses and artificial irrigation canals without sufficient treatment. River water quality analysis results showed that COD_{cr} is the most important contaminant in the Majia River, with more than 200 mg/L COD_{cr} in the Majia River mainstream (Cao *et al.* 2009).

Long-term irrigation of contaminated water would certainly threaten groundwater quality. To ensure groundwater quality in the Haihe River basin, the local government should first focus their efforts on standardization installation and control of discharge outlets and improve urban sewage treatment capacity and efficiency. In addition, we observed samples with high scores of concentrates at the administrative boundary between Henan and Hebei provinces. Cross-administrative region water pollution has always been a hotspot and problem in cross-boundary basin water resources utilization, water environmental programming, and water pollution prevention and control. Regulation sluices over irrigation canals at the boundary block surface water flow. Thus, contaminated water stagnates in the lower reaches, thereby preventing pollutant degradation and facilitating microbe proliferation. Lateral seepage of contaminated river water brings contaminants from surface water into the underground aquifer. The only way to avoid and protect the groundwater in these regions from contamination is by strengthening cross-regional collaboration, developing water resources, and protecting water quality.

CONCLUSION

Owing to large amounts of irrigation water not only changing local hydraulic conditions, but also transporting chemical substances in irrigation water and the vadose zone to groundwater aquifers, the groundwater chemistry in an irrigation region is much more complicated than the natural system. Studying the groundwater chemistry characteristics and its controlling geochemical processes is vital to learn the influence of irrigation practices on groundwater and to establish reasonable water resources management measures.

In this study, FA combined with ionic ratio method were used to identify the main geochemical processes controlling groundwater chemistry in PYR irrigation region; approximately three-quarters of the total variance of the data sets was explained by the four extracted factors. Factor 1 is composed of Ca^{2+}, Mg^{2+}, Sr^{2+}, and EC, and reflects natural hydrogeochemical processes and intensity of water–soil/rock interactions. Factor 3, marked by strong correlation of Na^{+} and HCO_3^{-}, represents another common and important hydrogeochemical processes – cation exchange process. Factors 1 and 3 are considered as natural factors that explained 41.69% of the total variation. Factor 2 is marked by strong correlation of NO_3^{-} and UV254, which are normally associated with human activities. Factor 4 is composed of Cl^{-} and K^{+}, which possibly indicated the influence of chemical fertilizers, especially those made from potash.

The areas affected by identified hydrogeochemical processes were determined by the factor scores of samples. Water–soil/rock interaction, especially dissolution of carbonate minerals were concentrated in the places away from river course and places with deeper groundwater. Cation exchange processes mainly occurred in regions with intensive irrigation activities and shallow groundwater. Therefore, irrigation activities should be encouraged in regions with high water hardness and deeper groundwater. This is because large amounts of fresh irrigation water can not only greatly dilute groundwater ion concentration, abundant Ca^{2+} in irrigation water diverted from the YR can also promote cation exchange process which is an important water-softening approach. In addition, a thick vadose zone can make local groundwater less susceptible to contamination.

Water samples with high Factor 2 and 4 scores are mainly concentrated in urban areas, confluence area of rivers, and administrative borders. This indicates that these regions are in vulnerable eco-environments and need to be paid more attention. In urban areas with a dense population and advanced industry, large amounts of municipal effluents and industrial wastewater beyond sewage treatment capacity are usually produced, which directly results in urban groundwater contamination. To solve this problem and protect urban groundwater resources, local government should make all efforts to improve sewage treatment ability, set up an all-sided emission supervision system, and draw up relevant rewards and punishment measures. For the confluence area of estuaries, pollution mainly results from the infiltration of contaminated river water, therefore the premise of groundwater protection in this area is preventing the river water from contamination. Once the surface water is contaminated, it will be difficult to avoid groundwater pollution. Water pollution in cross-administrative regions has always been a hotspot and should be settled through bilateral friendly negotiation and proper coordination of the higher administrative departments.

ACKNOWLEDGEMENTS

The research is supported by the Key Project for the Strategic Science Plan in IGSNRR, CAS (Grant No. 2012ZD003), the National Natural Science Foundation of China (Grant No. 41671027), and the National Basic Research Program (973 Program) of China (No. 2010CB428805).

REFERENCES

Appelo, C. A. J. 1996 Multicomponent ion exchange and chromatography in natural systems. In: *Reviews in Mineralogy,* Vol. 34 (P. C. Lichtner, C. I. Steefel & E. H. Oelkers, eds). Mineralogical Society of America, Washington, DC, USA, pp. 193–227.

Appelo, C. A. J. & Postma, D. 2005 *Geochemistry, Groundwater and Pollution,* 2nd edn. A.A. Balkema, Leiden, The Netherlands.

Brindha, K. & Elango, L. 2011 Fluoride in groundwater: causes, implications and mitigation measures. In: *Fluoride Properties, Applications and Environmental Management* (S. D. Monroy, ed.). Nova Science Publishers, Hauppauge, New York, USA, pp. 111–136.

Cao, J., Zhang, B. & Liu, Y. 2009 Water quality assessment and agro-ecological safety research in Majia River. *Environ. Sci. Manage.* **34** (7), 121–123 (in Chinese).

Carlyle, G. C. & Hill, A. R. 2001 Groundwater phosphate dynamics in a river riparian zone: effects of hydrologic flowpaths, lithology and redox chemistry. *J. Hydrol.* **247** (3–4), 151–168.

Cerling, T. E. & Pederson, B. L. 1989 Sodium-calcium ion exchange in the weathering of shales: implications for global weathering budgets. *Geology* **17**, 552–554.

Chapman, C. 1996 *Water Quality Assessments: A Guide to Use of Biota, Sediments and Water in Environmental Monitoring.* Chapman and Hill, London, UK.

Chen, J., He, D. & Cui, S. 2003 The response of river water quality and quantity to the development of irrigated agriculture in the last 4 decades in the Yellow River Basin, China. *Water Resour. Res.* **39** (3), 1047–1057.

Cloutier, V., Lefebvre, R., Therrien, R. & Savard, M. M. 2008 Multivariate statistical analysis of geochemical data as indicative of the hydrogeochemical evolution of groundwater in a sedimentary rock aquifer system. *J. Hydrol.* **353** (3–4), 294–313.

Davis, J. C. 2002 *Statistics and Data Analysis in Geology,* 3rd edn. John Wiley & Sons, New York, USA.

Deshmukh, S., Singh, A., Datta, S. & Annapurna, K. 2011 Impact of long-term wastewater application on microbiological properties of vadose zone. *Environ. Monitor. Assess.* **175** (1–4), 601–612.

Dragon, K. 2006 Application of factor analysis to study contamination of a semi-confined aquifer (Wielkopolska Buried Valley aquifer, Poland). *J. Hydrol.* **331** (1–2), 272–279.

Fenech, C., Rock, L., Nolan, K., Tobin, J. & Morrissey, A. 2012 The potential for a suite of isotope and chemical markers to differentiate sources of nitrate contamination: a review. *Water Res.* **46** (7), 2023–2041.

Gibbs, R. J. 1970 Mechanisms controlling world water chemistry. *Science* **170** (3962), 1088–1090.

Hem, J. D. 1985 *Study and Interpretation of the Chemical Characteristics of Natural Water,* 3rd edn. US Geological Survey, Water Supply Paper 2254.

Jankowski, J. & Acworth, R. I. 1997 Impact of debris-flow deposits on hydrogeochemical processes and the development of dryland salinity in the Yass River catchment, New South Wales, Australia. *Hydrogeology J.* **5** (4), 71–88.

Kass, A., Gavrieli, I., Yechieli, Y., Vengosh, A. & Starinsky, A. 2005 The impact of freshwater and wastewater irrigation on the chemistry of shallow groundwater: a case study from the Israeli Coastal Aquifer. *J. Hydrol.* **300** (1–4), 314–331.

Lawrence, F. W. & Upchurch, S. B. 1982 Identification of recharge areas using geochemical factor analysis. *Ground Water* **20** (6), 680–687.

Li, F., Pan, G., Tang, C., Zhang, Q. & Yu, J. 2008 Recharge source and hydrogeochemical evolution of shallow groundwater in a complex alluvial fan system, southwest of North China Plain. *Environ. Geol.* **55** (5), 1109–1122.

Meybeck, M. 1987 Global chemical-weathering of surficial rocks estimated from river dissolved loads. *Am. J. Sci.* **287** (5), 401–428.

Munoz-Carpena, R., Ritter, A. & Li, Y. C. 2005 Dynamic factor analysis of groundwater quality trends in an agricultural area adjacent to Everglades National Park. *J. Contam. Hydrol.* **80** (1–2), 49–70.

Panda, U. C., Sundaray, S. K., Rath, P., Nayak, B. B. & Bhatta, D. 2006 Application of factor and cluster analysis for characterization of river and estuarine water systems – a case study: Mahanadi River (India). *J. Hydrol.* **331** (3–4), 434–445.

Peng, X. 2012 Study on chemical fertilizer consumption and application effect on wheat and maize in Henan Province. Master Thesis, Henan Agricultural University, Kaifeng, China (in Chinese).

Prasanna, M. V., Chidambaram, S. & Srinivasamoorthy, K. 2010 Statistical analysis of the hydrogeochemical evolution of groundwater in hard and sedimentary aquifers system of Gadilam River Basin, South India. *J. King Saud Univ. Sci.* **22** (3), 133–145.

Qin, D., Qian, Y., Han, L., Wang, Z., Li, C. & Zhao, Z. 2011 Assessing impact of irrigation water on groundwater recharge and quality in arid environment using CFCs, tritium and stable isotopes, in the Zhangye Basin, Northwest China. *J. Hydrol.* **405** (1–2), 194–208.

Rajmohan, N. & Elango, L. 2004 Identification and evolution of hydrogeochemical processes in the groundwater environment in an area of the Palar and Cheyyar River Basins, Southern India. *Environ. Geol.* **46** (1), 47–61.

Rao, Y. 2009 Trend analysis of groundwater funnel in Puyang-Qingfeng-Nanle shallow aquifer. *Henan Water Resources & South to North Water Diversion* **1**, 27–28 + 37 (in Chinese).

Rogers, R. J. 1989 Geochemical comparison of ground water in areas of New England, New York, and Pennsylvania. *Ground Water* **27** (5), 690–712.

Stigter, T. Y., van Ooijen, S. P. J., Post, V. E. A., Appelo, C. A. J. & Carvalho Dill, A. M. M. 1998 A hydrogeological and hydrochemical explanation of the groundwater composition under irrigated land in a Mediterranean environment, Algarve, Portugal. *J. Hydrol.* **208** (3–4), 262–279.

Surinaidu, L. 2016 Role of hydrogeochemical process in increasing groundwater salinity in the central Godavari delta. *Hydrol. Res.* **47** (2), 373–389.

Tong, C., Wu, J., Miao, J., Liu, J. & Yu, S. 2005 A study of the development and water quality evolution of groundwater in the Northern Henan Plain. *Hydrogeol. Eng. Geol.* **5**, 13–16 (in Chinese).

Wang, H. 2007 Study on the water supply scale variation and its influencing factors in the lower Yellow River. Master Thesis, Xi'an University of Technology, Xi' an, China.

Yang, P., Yuan, D., Yuan, W., Kuang, Y., Jia, P. & He, Q. 2010 Formations of groundwater hydrogeochemistry in a karst system during storm events as revealed by PCA. *Chinese Sci. Bull.* **55** (14), 1412–1422.

First received 2 May 2016; accepted in revised form 21 August 2016. Available online 31 October 2016